Available online at www.sciencedirect.com
ScienceDirect
Catalysis Today 130 (2008) 14–23
CATALYSIS TODAY
www.elsevier.com/locate/cattod

Highly active MoS_2, $CoMoS_2$ and $NiMoS_2$ unsupported catalysts prepared by hydrothermal synthesis for hydrodesulfurization of 4,6-dimethyldibenzothiophene

Boonyawan Yoosuk [a,b], Jae Hyung Kim [a], Chunshan Song [a,*], Chawalit Ngamcharussrivichai [b], Pattarapan Prasassarakich [b]

[a] *Clean Fuels and Catalysis Program, The Energy Institute, and Department of Energy and Mineral Engineering, The Pennsylvania State University, University Park, PA 16802, USA*
[b] *Department of Chemical Technology, Faculty of Science, Chulalongkorn University, Bangkok 10330, Thailand*

Available online 14 September 2007

Abstract

This paper reports on a comparative study of unsupported MoS_2 and Me/MoS_2 (Me = Co, Ni) catalysts prepared by hydrothermal synthesis in our laboratory. Hydrothermal synthesis using water and organic solvent under hydrogen was found to produce highly active Mo based sulfide nano-size particles. MoS_2 had high surface area (320 m^2/g) and large pore volume (0.72 m^3/g). Addition of Co or Ni promoter decreased surface area and pore volume. Compared to MoS_2, downward shifts of the reduction temperatures were observed in TPR for Co(Ni)–Mo–S sulfides which suggested a decrease in metal sulfur bond strength. HRTEM and XRD results showed that MoS_2 formed large crystallized particles but the particle growth was inhibited when promoters were incorporated. For HDS, 4,6-dimethyldibenzothiophene (4,6-DMDBT) was slightly more reactive than dibenzothiophene (DBT) over the MoS_2. The liquid-phase adsorption showed that 4,6-DMDBT had higher capacity and stronger interaction with the adsorption site on MoS_2 than DBT. In distinct contrast to MoS_2, the promoted NiMo or CoMo sulfide showed higher liquid-phase adsorption selectivity for DBT than for 4,6-DMDBT. The promoter increased activity of MoS_2 and changed the contribution of the direct-desulfurization and of hydrogenation pathways. The adsorption and HDS results indicated that promoter affects both the number and the activity of active sites of the Mo sulfides. HDS activity of the unsupported Mo based sulfides was much higher than that of the sulfided commercial Co(Ni)Mo/Al_2O_3 catalysts.

Keywords: Unsupported catalyst; MoS_2; Promoter; Ni–Mo–S; Co–Mo–S; Hydrodesulfurization; Hydrothermal synthesis; Adsorption

1. Introduction

Catalysts based on molybdenum (Mo) have been used extensively for hydrodesulfurization (HDS) in petroleum refining for several decades and increasing attention is directed towards more effective catalysts for deep desulfurization [1–3]. The increase in the HDS activity by addition of Co or Ni into Mo catalyst has attracted the most attention in the studies of HDS catalysts. The synergetic effects of promoters on the activity of the Mo sulfides have been reported in the literatures [1,4,5]. The effect of promoter in Mo sulfide catalysts has been attributed to the amount of promoter atoms that can be accommodated on the edges of MoS_2 layers and also to the electronic transfer that promoter atom induces on Mo atoms located at these sites [6,7]. The exact nature of active sites in Co–Mo or Ni–Mo sulfide catalysts is still a subject of debate, but the Co–Mo–S model or Ni–Mo–S model is currently the one most widely accepted [1,8]. According to the model, the Co–Mo–S structure or Ni–Mo–S structure is responsible for the catalytic activity of the Co-promoted or Ni-promoted MoS_2 catalyst.

Recently, unsupported molybdenum based sulfide catalysts synthesized by using thiosalts as precursors showed high activity [9–13]. These Mo sulfide catalysts can be synthesized directly via a thermal decomposition method of ammonium tetrathiomolybdate (ATTM) and do not need further sulfidation. The Mo sulfide generated from decomposition of ATTM is more active than that from sulfidation of molybdenum oxide or

* Corresponding author. Tel.: +1 814 863 4466; fax: +1 814 865 3573.
E-mail address: csong@psu.edu (C. Song).

0920-5861/$ – see front matter © 2007 Elsevier B.V. All rights reserved.
doi:10.1016/j.cattod.2007.07.003

the reagent MoS_2, and thus ATTM has been used as catalyst precursor for generation of active MoS_2 catalyst. Recently, the new method for preparing highly dispersed unsupported Mo sulfide was reported by Song et al. [14–16]. This method is comprised of decomposing ATTM in water with added organic solvent under H_2 pressure. These MoS_2 catalysts with high surface area (342 m^2/g) had high activity for the cleavage of C–C bond and hydrogenation of naphthalene.

The purpose of this work is to study the effect of Co and Ni on the HDS activity of unsupported Mo sulfide catalysts prepared by hydrothermal method using ATTM for the simultaneous HDS of DBT and 4,6-DMDBT. The promoter effect on catalyst morphology is also studied. The liquid-phase adsorption was used to compare sulfur compound adsorption capacity, selectivity and mechanism of the unsupported Mo based sulfide catalysts, which may offer a new alternative to study the adsorption pattern of sulfur compounds on active sites of the Mo based sulfide catalysts.

2. Experimental

2.1. Preparation of catalysts

The unsupported Mo based sulfide catalysts were synthesized by using hydrothermal method. High-purity ammonium tetrathiomolybdate ($(NH_4)_2MoS_4$), nickel nitrate hexahydrate ($Ni(NO_3)_2{\cdot}6H_2O$) and cobalt nitrate hexahydrate ($Co(NO_3)_2{\cdot}6H_2O$) were purchased from Aldrich Chemical Company and were used without further purification. The catalyst synthesis was carried out in a batch reactor with a volume of 25 mL. 0.06 g of ATTM was dissolved in 10 g of deionized water and 1 g of organic solvent (decalin) was then added to this solution. 0.05 g of $Co(NO_3)_2{\cdot}6H_2O$ or $Ni(NO_3)_2{\cdot}6H_2O$ was dissolved in the minimum amount of water and was added to the solution to give an atomic ratio of Me/(Me + Mo) equal to 0.43 (Me = Ni or Co). The reactor was purged, then pressurized with hydrogen gas to a desired initial pressure (2.8 MPa) and placed in a preheated fluidized sand bath at 350 °C. After 2 h, the reactor was removed from the sand bath and immediately quenched in water bath. The unsupported catalysts synthesized were separated and immerged under an organic solvent.

The commercial supported catalysts $CoMo/Al_2O_3$ (Cr344) and $NiMo/Al_2O_3$ (Cr424) obtained from the Criterion Catalyst Company were used to compare the activity with the synthesized unsupported Mo based sulfide catalysts for the HDS of 4,6-DMDBT and DBT. The catalysts were crushed to a particle size of <1 mm and presulfided at 350 °C for 4 h in a flow of 5 vol.% H_2S/H_2 at flow rate of 150 mL/min. These sulfide catalysts were subsequently stored in decalin to minimize oxidation. The specific surface areas of Cr344 and Cr424 are 183.3 and 163.2 m^2/g, respectively.

2.2. Characterization of catalysts

The N_2 adsorption and desorption isotherms were measured on a Micromeritics ASAP 2020 instrument. Pore size distributions of the samples were determined from the isotherms by the Barrett–Joyner–Hallenda (BJH) method. Fresh samples were vacuum dried before the adsorption measurement. Temperature-programmed reduction (TPR) was conducted with a Micromeritics AutoChem 2910 instrument in Materials Research Laboratory. About 0.1 g of sample was charged in the reactor and heated up to 500 °C at the rate of 10 °C/min, held at 500 °C for 30 min and cooled to room temperature under Ar flow to remove the adsorbed materials. A mixture of 4.8 vol.% H_2/Ar was introduced at 50 mL/min into the sample loop. The heat treated sample was heated at a rate of 10 °C/min to 650 °C. The effluent gas was passed through a viscous solution of isopropanol cooled by liquid N_2 to remove the water produced during reduction and analyzed using a thermal conductivity detector. The X-ray diffraction (XRD) patterns were obtained on a Scintag Powder Diffractometer with Cu Kα emission, 30 mA 35 KV with a scanning speed of 2°/min. The diffractograms were analyzed using the standard JCPDS files. The high resolution transmission electron microscopy (HRTEM) was performed on a JEOL JEM-2010F transmission electron microscope. A small amount of sample was ground with a mortar and pestle. The sample was then suspended in ethanol and sonicated. A drop of the suspension was put on a lacey carbon film supported by a Cu grid.

2.3. System and procedure for liquid-phase adsorption

In order to compare the DBT and 4,6-DMDBT adsorption capacity of unsupported Mo, CoMo and NiMo sulfide catalysts, a fixed-bed adsorption system was used. The adsorption experiment was carried out at ambient temperature and pressure without using H_2 gas. The unsupported catalyst was packed in a stainless steel column having a bed dimension of 4.6 mm i.d. and 37.5 mm length. The model fuel contained 0.045 mol% of DBT and 0.045 mol% of 4,6-DMDBT in decalin was sent into the column by HPLC pump, flowed up through the bed at a liquid hourly space velocity (LHSV) of 1.04 h^{-1}. The effluent from the top of the column was collected periodically for quantitative analysis.

2.4. Catalytic activity and selectivity for hydrodesulfurization

A simultaneous HDS of DBT and 4,6-DMDBT was carried out in a horizontal micro-reactor (25 mL). The reactor was charged with the synthesized catalyst (0.023 g) and 4 g of reactant mixture (0.4 mol% of 4,6-DMDBT and 0.4 mol% of DBT in decalin). The sealed reactor was purged with hydrogen and then pressurized up to 2.1 MPa and placed in a fluidized sand bath which was preheated up to 300 °C. The reactor was agitated vertically at a rate of 200 strokes/min. The temperature inside the reactor was monitored by a thermocouple. After the reaction, the reactor was removed from the sand bath and immediately quenched in a cold-water bath. Finally, liquid products and the catalysts were collected. The liquid products were analyzed qualitatively with a Shimadzu GC/MS (GC12A/QP-500) and quantitatively with a Hewlett Packard GC-FID (HP5890) with a XTI-5 column (Restek). Both GC/MS and

GC-FID were programmed from 55 to 240 °C at heating rate of 5 °C/min.

3. Results

3.1. Catalyst characterizations

Table 1 presents the physical properties of unsupported Mo based sulfide catalysts. The surface area of catalysts was measured before the HDS reaction. The unsupported Mo sulfide catalyst had high surface area (320 m^2/g) and large pore volume (0.72 cm^3/g). After the addition of promoters, a significant decrease in the surface area and pore volume was observed. The NiMo and CoMo sulfide catalysts have the surface area of 201 and 196 m^2/g, respectively. These results indicate that the promoter addition influences the surface area of the unsupported Mo sulfide. The variation of surface areas of MoS_2 catalysts can be in the range of few to several hundred square meters per gram depending on the precursor and condition of the synthesis [17,18]. Alonso et al. [19] and Siadati et al. [20] reported that MoS_2 catalysts prepared from tetraalkylammonium thiomolybdates had surface area in the range of 60–329 and 170–225 m^2/g, respectively.

Fig. 1 presents the TPR profiles of the unsupported MoS_2, $CoMoS_2$ and $NiMoS_2$ catalysts. The TPR profiles of all catalysts showed a well-separated peak at low temperature and one or two broad peaks at high temperature. For unsupported MoS_2 catalyst, two main peaks were observed at 235 and 524 °C, respectively. After the incorporation of promoters (Co and Ni) into MoS_2 catalyst, the TPR profile shifted to lower temperatures for both low-temperature and high-temperature peaks. The position of the peak maxima/minima depends on the type of promoter. For the CoMo sulfide catalyst, the maximum reduction temperature was observed as a broad band centered between 383 and 424 ° and a low temperature peak at 198 °C. For the NiMo sulfide catalyst, three peaks were observed at 206, 366 and 439 °C, respectively. The addition of Co and Ni causes a significant downward shift (37 and 29 °C, respectively) in the peak position relative to low-temperature TPR peak of the unpromoted MoS_2 catalyst (235 °C) indicating that the addition of promoter enhanced the reducibility of Mo sulfide.

Fig. 2 presents the XRD patterns for the unsupported Mo sulfide catalysts before and after addition of promoters. As compared to a commercial MoS_2 powder, both unpromoted and promoted Mo sulfide catalysts exhibit weak XRD peaks, indicating a very poorly crystalline structure characteristic of the molybdenum disulfide. The XRD peaks became broader

Table 1
Composition and properties of fresh unsupported Mo based sulfide catalysts

Catalysts	Me/(Mo + Me)[a]	Surface area[b] (m^2/g)	Pore volume (cm^3/g)
MoS_2	0.00	320	0.72
$NiMoS_2$	0.43	201	0.28
$CoMoS_2$	0.43	196	0.27

[a] Me/(Mo + Me) molar ratio based on metal in the precursor salts (Me = Co or Ni).
[b] Samples were vacuum dried before surface area measurement.

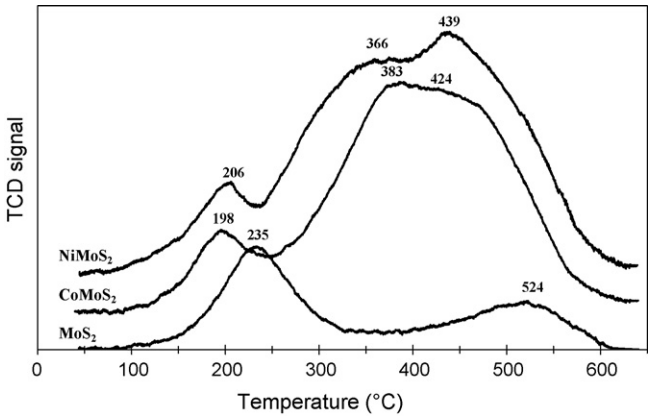

Fig. 1. TPR patterns of unsupported MoS_2, $CoMoS_2$ and $NiMoS_2$ catalysts.

when the (Ni or Co) promoter was added. The intensity of most MoS_2 peaks were significantly decreased and particularly for the unsupported CoMo sulfide, the peak at $2\theta = 14.4°$, characteristic of the (0 0 2) basal planes of crystalline MoS_2 became very low. In the sulfides with promoters, the diffractions of separate Ni and Co sulfides were detected due to high loading amount of these metals and the crystallized Ni_3S_4 and Co_9S_8 were formed. For the promoted sulfide catalysts, the Ni–Mo–S or Co–Mo–S phases were not reflected by any major XRD peaks. The active structure (Ni–Mo–S or Co–Mo–S phase) possibly presents as small nano-sized particles, which cannot be detected by XRD method [21].

Fig. 3 presents the HRTEM photographs of unsupported Mo sulfide catalysts with and without Ni promoter. The black thread-like fringes in Fig. 3 correspond to the MoS_2 slabs. The fringes observed in the photographs had a spacing of about 0.65 nm that was the characteristic of (0 0 2) basal planes of crystalline MoS_2. The TEM images clearly showed that the unpromoted MoS_2 catalyst had long slabs. The curvature of slabs increased while the slab length decreased upon the addition of Ni promoter. The number of the stacked layer of Ni promoted MoS_2 catalyst was more than that of the unpromoted catalyst. It can be concluded that the incorporation of nickel in to the Mo sulfide catalyst increases the number of stacked layer,

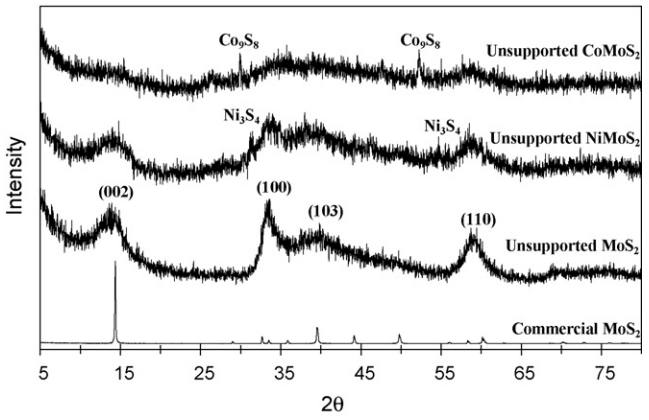

Fig. 2. XRD patterns of unsupported Mo based sulfide catalysts and commercial MoS_2.

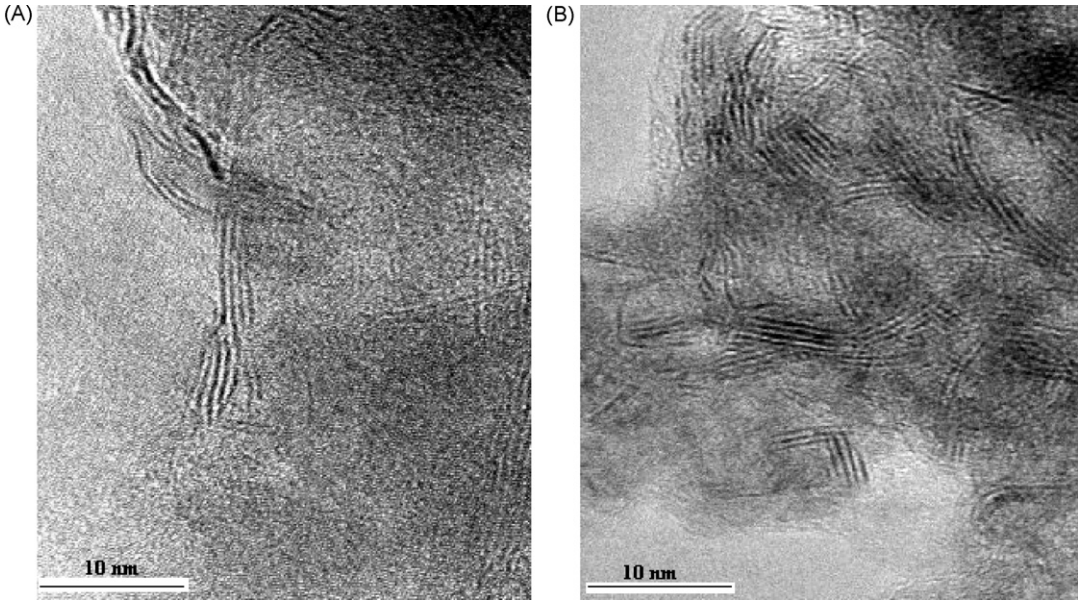

Fig. 3. High-resolution TEM images of unsupported catalysts: (A) MoS_2; (B) $NiMoS_2$.

while decreases the crystallite size of catalyst. The TEM images also indicated that the smaller particles were formed when the promoters were incorporated with the Mo sulfide.

3.2. Catalytic activity and selectivity for simultaneous HDS of DBT and 4,6-DMDBT

The simultaneous HDS of 4,6-DMDBT and DBT was carried out to examine the activity of the catalysts. Pseudo-first-order rate constants were determined using the method reported in our recent kinetic study [22]. The rate constants of simultaneous HDS of DBT and of 4,6-DMDBT over the unsupported MoS_2, $NiMoS_2$ and $CoMoS_2$ catalysts and commercial NiMo and CoMo alumina supported catalysts are shown in Fig. 4. Surprisingly, the activity of MoS_2 catalyst for HDS of 4,6-DMDBT was higher than that of DBT as shown in Table 2 (297.7×10^{-5} s^{-1} g cat^{-1} for 4,6-DMDBT and 166.3×10^{-5} s^{-1} g cat^{-1} for DBT). Although, for the unsupported Mo sulfide

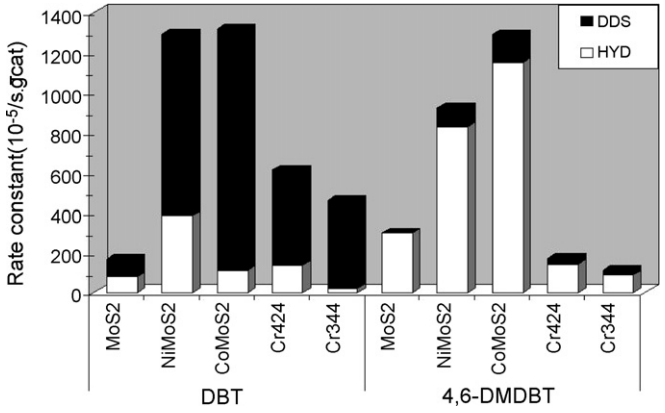

Fig. 4. HDS rate constants for simultaneous HDS of DBT and 4,6-DMDBT over the unsupported MoS_2, $NiMoS_2$ and $CoMoS_2$ catalysts and commercial alumina-supported NiMoS (Cr424) and CoMoS (Cr344) catalysts.

catalyst, the rate constant of direct-desulfurization (DDS) pathway and that of hydrogenation (HYD) pathway were similar for DBT HDS, the rate constant of HYD pathway was clearly higher than that of DDS pathway for 4,6-DMDBT HDS. The selectivity of HYD pathway was almost equal to one for HDS of 4,6-DMDBT as shown in Table 2. This result indicated that the unpromoted Mo sulfide catalyst possessed high hydrogenation activity.

The NiMo and CoMo sulfide catalysts had higher activity than the Mo sulfide catalyst. As shown in Table 2, the promoting effect was around 8 for DBT HDS and 4 for 4,6-DMDBT HDS. The activity of unsupported $CoMoS_2$ catalyst was higher than that of $NiMoS_2$ catalyst for 4,6-DMDBT HDS but was almost the same for DBT HDS. For 4,6-DMDBT HDS, the promoter caused the increase in DDS pathway selectivity while did not change the HYD pathway selectivity. For DBT HDS, the promoter also gave the increase in DDS pathway selectivity while decreased the HYD pathway selectivity. Therefore, over the promoted Mo sulfide catalysts, DDS pathway became the main pathway for the HDS of DBT and HYD pathway was the predominant pathway for 4,6-DMDBT HDS. From Table 2, it is obvious that the promoter not only increased the catalytic activity of the Mo sulfide catalyst but also changed the contribution on the DDS and the HYD pathways for both DBT and 4,6-DMDBT HDS. The promoting effect on the HYD pathway was much less than that on the DDS pathway for both 4,6-DMDBT and DBT HDS. These results indicate that the promoting effect was essentially due to the enhancement of the rate of DDS pathway (or the C–S bond cleavage activity in general).

Fig. 4 presents that the activities of unsupported Mo based sulfide catalysts prepared from hydrothermal method were consistently higher than that of the commercial NiMo and CoMo alumina supported catalysts. More significantly, the HDS activity of the unsupported catalysts was five times the

Table 2
Activity and selectivity of unsupported MoS_2, $NiMoS_2$ and $CoMoS_2$ catalysts for simultaneous HDS of DBT and 4,6-DMDBT

	S compounds					
	DBT			4,6-DMDBT		
	MoS_2[a]	$NiMoS_2$[a]	$CoMoS_2$[a]	MoS_2[a]	$NiMoS_2$[a]	$CoMoS_2$[a]
$k_1 + k_2$ (10^{-5}/s g_{cat})	166.3	1290.0	1316.4	297.7	920.5	1289.5
k_1/k_2	0.9	0.4	0.1	170.4	8.8	8.1
$k_{1(HYD)}$ (10^{-5}/s g_{cat})	78.2	381.9	111.1	295.9	826.5	1147.8
$k_{2(DDS)}$ (10^{-5}/s g_{cat})	88.1	908.1	1205.3	1.7	94.0	141.7
Selectivity						
S HYD	0.47	0.30	0.08	0.99	0.90	0.89
S DDS	0.53	0.70	0.92	0.01	0.10	0.11
Promoting effect						
Total	1.0	7.8	7.9	1.0	3.1	4.3
On HYD	1.0	4.9	1.4	1.0	2.8	3.9
On DDS	1.0	10.3	13.7	1.0	54.3	81.6

[a] Catalysts.

commercial catalysts for 4,6-DMDBT HDS. Although the unsupported Mo sulfide had lower activity for DBT HDS, it had higher activity for HDS of 4,6-DMDBT as compared to the commercial catalysts. This might be explained by the high hydrogenation activity of the Mo sulfide catalyst and HYD pathway is the main path way for 4,6-DMDBT HDS. Both unsupported and commercial catalysts showed the same trend that the DDS pathway was the main pathway for DBT HDS and the HYD pathway was predominant pathway for HDS of 4,6-DMDBT. The activity of $NiMo/Al_2O_3$ catalyst was higher than that of the $CoMo/Al_2O_3$ catalyst for HDS of both sulfur compounds. Interestingly, the unsupported NiMo and CoMo sulfide catalysts had the same activity for DBT HDS while the CoMo sulfide catalyst had higher activity than NiMo sulfide catalyst for HDS of 4,6-DMDBT.

3.3. Simultaneous liquid-phase adsorption of DBT and 4,6-DMDBT

The liquid-phase adsorption of 4,6-MDBT and DBT over the unsupported Mo sulfide catalyst was conducted at ambient temperature and ambient pressure. The breakthrough curves of both sulfur compounds are shown in Fig. 5. No detectable sulfur was found until the amount of liquid fuel flow reached 4.2 g of the treated fuel per gram of catalyst packed in the bed (g-F/g-C), indicating that both 4,6-DMDBT and DBT were adsorbed on the catalyst and thus removed from the liquid fuel. The first breakthrough compound was DBT with the breakthrough amount of 4.2 g-F/g-C. After the breakthrough, the C/C_0 value (a ratio of the outlet concentration to the initial concentration in the model fuel) for the DBT increased to over 1.0. After the saturation point, the C/C_o value increased gradually to 1.12 and returned to 1.0 at the treated fuel amount of 25.2 g-F/g-C. When the treated fuel per gram of catalyst increased to 5.9 g-F/g-C, 4,6-DMDBT was detected in treated fuel. Then, the C/C_0 value of 4,6-DMDBT increased slowly and reached the saturation point at the treated fuel amount per gram of catalyst of 55.2 g-F/g-C. The breakthrough, saturation and net capacities for both sulfur compounds were calculated and listed in Table 3. According to the breakthrough order, it is interesting that 4,6-DMDBT was adsorbed more than DBT over the unsupported Mo sulfide. The net capacity of 4,6-DMDBT was about 2.1 times higher than that of DBT.

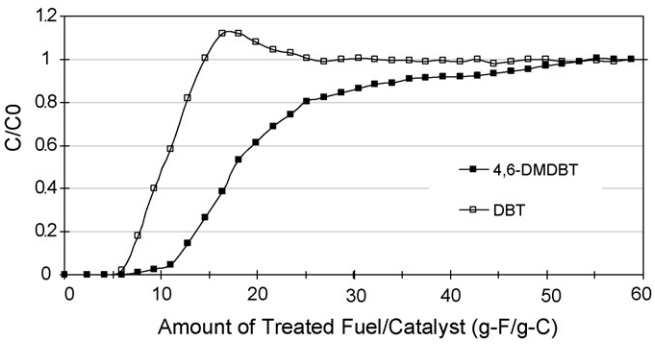

Fig. 5. Breakthrough curves for the liquid-phase adsorption of 4,6-DMDBT and DBT at ambient temperature and pressure over the unsupported Mo sulfide catalyst.

Table 3
Liquid-phase adsorption capacities (mmol/g) of three unsupported catalysts for DBT and 4,6-DMDBT on the basis of GC-FID analysis

	DBT	4,6-DMDBT	Total
MoS_2			
Breakthrough	0.014	0.019	0.033
Saturation	0.033	0.068	0.101
Net[a]	0.032	0.068	0.100
$NiMoS_2$			
Breakthrough	0.018	0.018	0.037
Saturation	0.061	0.049	0.110
Net[a]	0.061	0.048	0.109
$CoMoS_2$			
Breakthrough	0.020	0.020	0.040
Saturation	0.064	0.056	0.120
Net[a]	0.064	0.056	0.120

[a] Net adsorption capacity when the adsorption was ended.

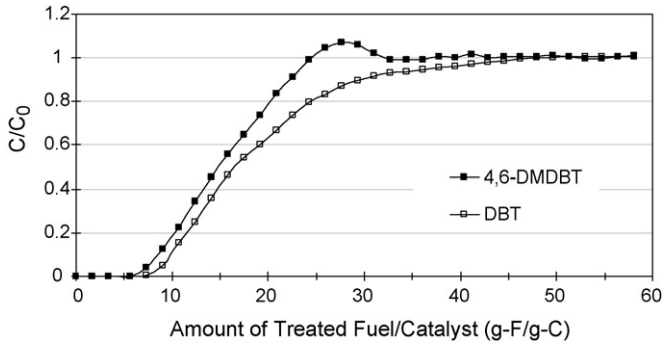

Fig. 6. Breakthrough curves for the liquid-phase adsorption of 4,6-DMDBT and DBT at ambient temperature and pressure over the unsupported NiMo sulfide catalyst.

The breakthrough curves of 4,6-DMDBT and DBT adsorption over the unsupported NiMo sulfide catalyst are shown in Fig. 6. No sulfur compound was detected when the treated fuel was less than 5.6 g-F/g-C. Unlike the unsupported Mo sulfide catalyst, 4,6-DMDBT and DBT broke through with the same breakthrough amount of the treated fuel. The breakthrough capacities for both compounds were 0.018 mmol/g. After the breakthrough, the C/C_0 value of 4,6-DMDBT increased reaching the maximum at 1.07 and then, returned to 1.0 at the treated fuel amount of 32.7 g-F/g-C. On the other hand, after the breakthrough, the C/C_0 value of DBT rose gradually and reached 1.0 at the treated fuel amount per gram of catalyst of 47.8. The net capacities of 4,6-DMDBT and DBT were 0.048 and 0.061 mmol/g, respectively.

The breakthrough curves of 4,6-DMDBT and DBT adsorption over the unsupported CoMo sulfide are shown in Fig. 7. Similar to the unsupported NiMo sulfide, 4,6-DMDBT and DBT broke through with the same breakthrough amount of the treated fuel (6.1 g-F/g-C). After the breakthrough, the C/C_0 value of both 4,6-DMDBT and DBT increased gradually and synchronously reached 1.0 almost at the same amount of treated fuel (52.3 g-F/g-C). However, the breakthrough curve of DBT showed more inclined than that of 4,6-DMDBT indicating that the amount of DBT adsorbed was greater that that of 4,6-DMDBT over the unsupported CoMo sulfide. The net capacities of 4,6-DMDBT and DBT were 0.056 and 0.064 mmol/g, respectively.

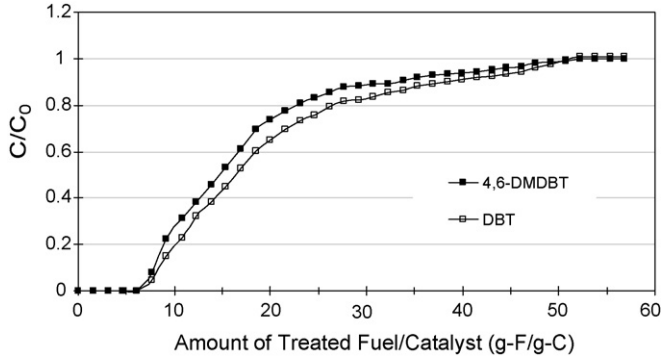

Fig. 7. Breakthrough curves for the liquid-phase adsorption of 4,6-DMDBT and DBT at ambient temperature and pressure over the unsupported CoMo sulfide catalyst.

4. Discussion

4.1. BET, TPR, XRD and HRTEM

The decomposition of thiosalts has been widely observed by thermal analysis [5,23,24] and MoS_2 is formed from thiosalt precursors according to the following reactions.

$$(NH_4)_2MoS_4 \rightarrow MoS_3 + (NH_4)_2S \quad (1)$$

$$MoS_3 \rightarrow MoS_2(\text{amorphous}) + 1/xS_x \quad (2)$$

$$MoS_2(\text{amorphous}) \rightarrow MoS_2(\text{crystalline}) \quad (3)$$

MoS_3 is formed and then transformed to a highly disordered (poorly crystalline) MoS_2 with the elimination of sulfur (or hydrogen sulfide, if excess hydrogen is present). Finally, a re-stacking of the MoS_2 crystallites takes place.

For the catalyst preparation, ATTM reacted with promoter (Co or Ni) in the environment of hydrogen to form the bimetallic sulfide catalyst as follows [4] which Me is Co or Ni.

$$2(NH_4)_2MoS_4 \rightarrow Me(NO_3)_2 \rightarrow (NH_4)_2\{Me(MoS_4)_2\} + 2NH_4NO_3 \quad (4)$$

There is bonding between thioanion and promoter cation in this step. In the presence of hydrogen, the bimetallic sulfide is formed as follows:

$$Me(MoS_4)_2 + H_2 \rightarrow Me(MoS_3)_2 + H_2S \quad (5)$$

$$Me(MoS_3)_2 + H_2 \rightarrow Me(MoS_2)_2 + H_2S \quad (6)$$

The chemical interaction among the promoter and Mo atoms indicates that a good dispersion of the promoter in MoS_2 is obtained resulting in the formation of a large number of CoMo or NiMo sites.

The addition of promoter to the unsupported Mo sulfide catalyst not only changed the catalytic activity but also the porosity and the morphology of the Mo based sulfide catalyst. These changes can be clearly seen from the surface area of three catalysts, the HRTEM images, even the shift of low-temperature TPR peak as well as the broader XRD peak when the promoter was added. These indicate that not only a chemical (such as edge decoration) but also a structural (such as textural or morphological) promoting effect is involved.

The BET surface area of the NiMo and CoMo sulfide was lower than that of the unpromoted Mo sulfide (Table 1). The phenomenon of the decrease in the surface area of sulfide catalyst due to the addition of promoter has been observed in earlier studies [23,25]. Pedraza and Fuentes [4] also reported that the surface area decreased from 50 to 20–30 m^2/g when the promoter was added into Mo sulfide catalyst. The relationship between specific surface areas and the HDS activity was not straightforward and the catalyst with larger surface area does not necessarily yield a higher HDS rate constant. This is in agreement with some studies that the catalytic activity of molybdenum sulfide catalysts was not directly related to BET surface area but dependent on the morphology of catalysts [1]. The lack of the correlation between BET surface area and HDS

activity over unsupported Mo based sulfide catalysts was earlier reported by Inamura and Prins [25] and Alvarez et al. [5].

The TPR profile of sulfide catalysts contains several well separated reduction peaks. The low-temperature peak can be assigned to surface sulfur atoms (weakly bonded sulfur) whereas the ''bulk reduction'' occurs in the higher temperatures range. In the low-temperature region, the surface is reduced and the coordinative unsaturated sites (CUS) are created which are believed to be responsible for the active sites [26]. For MoS_2, apparently, the well separated low-temperature peak at 235 °C originates from sulfur atoms that are weakly bound on the catalyst surface. The signal above 327 °C corresponds to the partial reduction of the small MoS_2 crystals [27,28]. The profile of this curve is similar to others presented in literature [29]. The behavior of this catalyst during TPR was proposed by Li et al. [30].

$$[MoS_2]_x\text{–}S \xrightarrow[<177\,^\circ C]{H_2} [MoS_2]_x + H_2S \quad \text{(surface)} \tag{7}$$

$$[MoS_2]_x \xrightarrow[<400\,^\circ C]{H_2} [MoS_2]_x\text{–}H \quad \text{(surface)} \tag{8}$$

$$[MoS_2]_x\text{–}H \xrightarrow[>300\,^\circ C]{H_2} [Mo_xS_{2x-1}]^* + H_2S \quad \text{(surface)} \tag{9}$$

$$MoS_2 \xrightarrow[>327\,^\circ C]{H_2} MoS^* + H_2S \quad \text{(mass)} \tag{10}$$

In these expression, $[MoS_2]_x$ represents MoS_2 on the surface and ''*'' represents an anionic vacancy.

The TPR results showed that the addition of Co or Ni to the unsupported Mo sulfide catalysts caused a significant downward shift of the first peak temperature during TPR. With the addition of promoter, the new TPR peaks in the high temperature range were observed. These new peaks were not contributed by separated sulfide phase of promoter since the reduction of bulk separated sulfide phase began around 527 °C and a peak maximum was observed at 677 °C, as reported in the literature [27], which is much higher than the TPR temperature of new peak observed in the present work. These TPR results suggest that there is an interaction between promoter and Mo species. The lower TPR peak temperatures for Co and Ni promoted unsupported Mo sulfide catalysts imply a lower sulfur binding energy as compared to unpromoted Mo sulfide catalyst. In other words, the promoter decreased the strength of the molybdenum–sulfur–promoter bond in the sulfide itself. This is consistent with the theoretically estimated metal-sulfur bond energies indicating that the addition of Co or Ni on MoS_2 should give rise to a lower metal sulfur bond strength [31,32]. It is generally believed for transition metal sulfide that sulfur vacancies created by means of reduction with hydrogen are responsible for the observed catalytic activity [1,21]. This formed the basis for the bond energy model in which there exists a correlation between the catalytic activity and the estimated metal sulfur bond strength [25]. It is clearly seen in the results that the promoted catalysts had much higher catalytic activity than unsupported Mo sulfide catalyst (Table 2). This activity variation can be rationalized in terms of the bond energy when the metal sulfur bond strengths are assessed by TPR peak temperature. This TPR result agrees with the work reported by Jacobsen et al. [29] who observed a converse relationship between the temperature of the first H_2S TPR peak of metal sulfides and the HDS activity of catalysts.

It is generally accepted that the promoter atom is located at the edges of the hexagonal MoS_2 platelets [33,34]. It is also believed that the Co–Mo–S structure or Ni–Mo–S structure is responsible for the catalytic activity of the Co-promoted or Ni-promoted MoS_2 catalyst in the HDS reaction [1,2,6]. As the promoter is added, it preferentially interacts with the edge of the MoS_2 crystallite surface and forms the active species.

The XRD pattern showed that the intensity of MoS_2 peaks were decreased significantly and particularly the peak at $2\theta = 14.4^\circ$, characteristic of the (0 0 2) basal planes of crystalline MoS_2 became very low on the unsupported CoMo sulfide. It indicated that much smaller size of (0 0 2) phase of MoS_2 was generated or/and Co or Ni places the phase of MoS_2, specifically on the (0 0 2) phase. This results in the decreasing of the length of the stack after the addition of promoter which was observed in HRTEM analysis as shown in Fig. 3. The XRD pattern and HRTEM images showed that the addition of promoter caused the decrease in the length of the basal planes and increase in average number of layers in the stacks. This result is in agreement with previous result showing that Co decoration at the edges of MoS_2 slabs can induce an increase of the stacking height [35]. HRTEM results agreed very well with XRD analysis. In the absence of the promoters, the MoS_2 formed large crystallized particles as seen from long length slab and narrow XRD pattern. The growth of MoS_2 crystallized particles was inhibited when the promoters are incorporated. The effect of promoter on the size of MoS_2 might be explained by the decoration of promoter at the edges of MoS_2 slabs which prevents the further growth of MoS_2 crystallites.

However, not all of the promoter added results in the formation of the Co–Mo–S or Ni–Mo–S species. When all of the edges are covered, the additional promoter could form a separate phase of the sulfide as seen in Fig. 2. The Ni_3S_4 and Co_9S_8 peaks were detected after the addition of Ni and Co promoter precursor to Mo precursor ATTM, respectively. What role does this separate metal sulfide play is a matter of debate. If these metal (Ni and Co) sulfide particles are indeed catalytically active, they might help adsorb and dissociate hydrogen molecule. The resulting H species could attack the MoS_2 particles and create coordinative unsaturated site at the edges [36,37].

4.2. Catalytic performance of the unsupported Mo, CoMo and NiMo sulfides

As many studies [38–40] indicated, the HDS of alkyldibenzothiophenes occurs through two parallel reactions: (1) the direct desulfurization (DDS) pathway which involves direct C–S bond cleavage without prior hydrogenation, possibly via chemisorption of the sulfur atom in the molecule on an exposed Mo ion at a sulfur vacancy site, followed by hydrogen transfer and sulfur elimination to complete desulfurization; and (2) the hydrogenation pathway (HYD) which involves aromatic ring

hydrogenation first, likely via the adsorption of sulfur compound on the MoS_2 stack through the π-electrons on the aromatic rings. This is followed by hydrogenation of one of the aromatic rings and sulfur elimination to complete desulfurization.

The ultimate goal is to synthesize catalysts for deep HDS that can remove the most refractory sulfur compounds such as 4,6-dialkyldibenzothiophenes. The results featured in Fig. 4 suggested that a unique feature of the unsupported Mo based sulfide catalysts prepared by hydrothermal method is their superiority over the commercial catalysts for the HDS of the refractory forms of sulfur compounds especially 4,6-DMDBT. The improved hydrodesulfurization activity due to the higher surface area of the unsupported catalysts (about 20–30 m^2/g higher than the commercial catalysts) is only a part of the reason for the superior performance of the unsupported Mo based sulfide catalysts. It is possible that the unsupported Mo based sulfide catalyst possesses an active phase that has superior intrinsic activity for HDS as compared to the commercial catalysts.

The rate constant of 4,6-DMDBT HDS was higher than that of HDS of DBT over the Mo sulfide catalyst. This is mainly due to a very high rate of the hydrogenation (HYD) pathway over this catalyst (47% for DBT and 99% for 4,6-DMDBT as shown in Table 2). It is probably explained by the higher adsorption capacity and stronger interaction of 4,6-DMDBT on active site of this catalyst which can be seen from the selective adsorption results (Fig. 5. and Table 3). However, as generally observed, DBT was more reactive than 4,6-DMDBT on the unsupported CoMo and NiMo catalysts. Unlike general catalysts, 4,6-DMDBT was not much less reactive than DBT over all of unsupported catalysts (approximately 0.8 times compare with 2–6 times as reported in the literature) [22,41]. From Table 2, it is clear that Co or Ni promoted Mo sulfide had higher activity than unpromoted Mo sulfide for both DBT and 4,6-DMDBT HDS. It might be explained by an increased electron density not only at the Mo atoms but also at the S atom when promoter were added in Mo sulfide as reported by Muller et al. [42]. Increasing the electron density at the S atom is expected to enhance both the activity of H_2 and the formation of more S vacancies which are believed to be the catalytic active sites [43].

Promoter also enhanced the rate constant of HYD and DDS pathways for both sulfur compounds. However, it increased the rate constant of the DDS pathway much more than that of the HYD pathway. This result is in agreement with previous results showing that Ni or Co promotion favors the DDS pathway [41,44,45]. This effect might be explained by an increase of the basicity of sulfur atoms shared between promoter Mo atoms [46]. If the C–S bond cleavage occurs through the attack of a hydrogen atom at the β position relative to the sulfur atom in the organic sulfur molecule by a sulfur anion acting as a basic site [41]. Thus, an increase of basicity would favor the C–S bond cleavage.

Table 4 presents the turn over frequency (TOF) of three unsupported catalysts for DBT and 4,6-DMDBT on the basis of adsorption site. The TOFs were calculated by using the adsorption capacities of three catalysts as a measurement of the number of active sites. The unpromoted Mo sulfide catalyst showed the lowest TOF values for both DBT and 4,6-DMDBT. The TOF values of promoted Mo sulfide catalyst increased up to 4 times unpromoted catalyst, indicating that the active site of the promoted Mo sulfide catalyst is intrinsically more active than that of the unpromoted Mo sulfide catalyst. The results showed clearly that the promoter affects not only the number of active sites but also the activity of active sites of the unsupported Mo sulfide catalyst.

Table 4
Turnover frequency (TOF) of three unsupported catalysts for DBT and 4,6-DMDBT on the basis of adsorption capacities

Catalyst	DBT (s^{-1})	4,6-DMDBT (s^{-1})
MoS_2	53	44
$NiMoS_2$	213	190
$CoMoS_2$	207	229

4.3. Comparison of adsorption capacity, selectivity and mechanism of the unsupported Mo, CoMo and NiMo sulfides

Typically, adsorption performance depends on both surface chemical properties (active sites and their density) and physical properties (surface area, pore size and distribution). The breakthrough curves of 4,6-DMDBT and DBT adsorption on the unsupported Mo, NiMo and CoMo sulfides showed different adsorptive selectivity for these different catalysts. The total adsorption capacities based on the catalyst weight increased in the order of CoMo > NiMo > Mo sulfide (as shown in Table 3). This order is consistent with the catalytic activity of these three catalysts. The unsupported Mo sulfide showed the highest adsorption capacity for 4,6-DMDBT and this capacity decreased after the addition of the promoter. On the other hand, the adsorption capacity for DBT increased when the Mo sulfide was promoted.

The adsorption behavior of sulfur compounds on the unsupported catalysts is similar to the work previously reported by Kim et al. [47]. After passing through the saturation point ($C/C_0 = 1$) the outlet concentration of some compounds increases continuously over its initial concentration in the model fuel reaching the maximum value and then, decreases gradually to the initial value. This phenomenon resulted from a partially reversible adsorption of that compound. Another reason is that the compounds have relatively lower adsorptive affinity than the subsequently breakthrough compounds, resulting in at least partial replacement of the compounds with lower adsorptive affinity by the compounds with higher adsorptive affinity. The net capacity was calculated by subtracting the area between the breakthrough curve and line $C/C_0 = 1$ after the saturation point which represents the amount of the replaced molecules from the area between the breakthrough curve of the compound and line $C/C_0 = 1$ before the saturation point which represents the amount of the adsorbed molecules.

The adsorption of sulfur compounds on the unsupported Mo sulfide showed that 4,6-DMDBT was adsorbed 2.1 times DBT

over Mo sulfide (Table 3). A part of the adsorbed DBT can be replaced by 4,6-DMDBT. This result indicated that the interaction of 4,6-DMDBT with the adsorption site is stronger than that of DBT. It is interesting to note that the methyl groups on the aromatic rings showed a significant promoting effect on the adsorption selectivity of Mo sulfide, indicating that the methyl groups enhance the adsorption affinity or interaction through increasing the electron density of the aromatic rings since the methyl substitutent leads to the increasing of π-electron density on the aromatic rings [48]. The adsorptive selectivity agreed very well with HDS reactivity of 4,6-DMDBT and DBT on the unsupported Mo sulfide catalysts. Higher adsorption capacity and stronger interaction of 4,6-DMDBT on active site probably cause the higher reactivity of 4,6-DMDBT than DBT over the unsupported Mo sulfide catalyst as shown in Fig. 4.

For the unsupported NiMo sulfide, the adsorptive selectivity of DBT was higher than that of 4,6-DMDBT which reversed the adsorptive selectivity order of the Mo sulfide. However, the replacement phenomenon was also observed in this catalyst. The amount of DBT adsorbed was greater than that of 4,6-DMDBT and a part of adsorbed 4,6-DMDBT can be replaced by DBT. Unlike on the Mo sulfide, the selective order showed that the methyl groups on the 4- and 6-position of DBT strongly inhibited the adsorption of 4,6-DMDBT on NiMo sulfide. This result indicated that a direct interaction between the sulfur atom and the adsorption site on the NiMo sulfide could play an important role in the selective adsorption of DBT and 4,6-DMDBT and the two methyl groups block the approach of the sulfur atom to the adsorption site.

Like adsorption on the NiMo sulfide, the amount of adsorbed DBT was slightly higher than that of adsorbed 4,6-DMDBT on the unsupported CoMo sulfide as shown in Table 3. Interestingly, both DBT and 4,6-DMDBT reached the saturation point almost at the same amount of treated fuel and the replacement phenomenon was not observed. This result suggested that the methyl groups on the aromatic ring shows some negative effect to the adsorption of the sulfur compounds on the CoMo sulfide and this effect is less strong than that on the NiMo sulfide. This adsorption selectivity might explain HDS result that the HDS reactivity of DBT and 4,6-DMDBT was not much different (Table 3).

5. Conclusions

The unpromoted and promoted Mo sulfide (unsupported) catalysts prepared by hydrothermal synthesis method have different properties and different HDS performance. Unsupported Mo sulfide catalyst showed high surface area without using any support material. The addition of promoters (Ni or Co) resulted in significant decrease in surface area and pore volume of unsupported Mo sulfide. However, on the basis of HRTEM and XRD analysis, the addition of promoters led to the increase in curvature of MoS_2 slabs and the decrease in slab length. This is probably because Ni or Co may be located on edge of MoS_2 structure and prevents the growth (or aggregation) of crystallite. These catalysts have higher content of Ni or Co as compared to conventional supported catalysts. A part of the added Co and Ni promoters may be present as Co sulfide and Ni sulfide, as also suggested by XRD. TPR showed that the addition of promoter to the unsupported Mo sulfide causes a significant downward shift of the first peak reduction temperature which suggests the decrease in the metal sulfur bond energy. The liquid-phase adsorption showed that different sulfides exhibit different adsorption capacity and selectivity towards 4,6-DMDBT and DBT, which reflect on the differences in adsorption sites on the catalyst surface. 4,6-DMDBT had higher adsorption capacity and stronger interaction with the active sites on the unsupported Mo sulfide than DBT. This might explain the interesting HDS result that 4,6-DMDBT showed higher HDS reactivity than DBT over the MoS_2 catalyst. In distinct contrast to MoS_2, the adsorption selectivity of DBT on the promoted NiMo or CoMo sulfide was higher than that of 4,6-DMDBT. These results indicated that the promoter not only increased the catalytic activity of the unsupported Mo based sulfide catalyst but also changed the contribution of the DDS and of HYD pathways, probably due to the change in the surface active sites.

Acknowledgments

We gratefully acknowledge the support of US Department of Energy, National Energy Technology Laboratory through the Refinery Integration program, US Environmental Protection Agency through NSF/EPA TSE program and the Thailand Research Fund through the Royal Golden Jubilee program. We thank Dr. Xiaoliang Ma of PSU for helpful discussion.

References

[1] H. Topsoe, B.S. Clausen, F.E. Massoth, in: J.R. Anderson, M. Boudart (Eds.), Catalysis Science and Technology, vol. 11, Springer, Berlin, 1996, p. 162.
[2] C.S. Song, Catal. Today 86 (2003) 211.
[3] C.S. Song, X.L. Ma, Appl. Catal. B: Environ. 41 (2003) 207.
[4] F. Pedraza, S. Fuentes, Catal. Lett. 65 (2000) 107.
[5] L. Alvarez, J. Espino, C. Ornelas, J.L. Rico, M.T. Cortez, G. Berhault, G. Alonso, J. Mol. Catal. A: Chem. 210 (2004) 105.
[6] R. Candia, B.S. Clausen, H. Topsoe, J. Catal. 77 (1982) 564.
[7] S. Harris, R.R. Chianelli, J. Catal. 98 (1986) 17.
[8] R. Prins, Adv. Catal. 46 (2001) 399.
[9] H. Nava, C. Ornelas, A. Aguilar, G. Berhault, S. Fuentes, G. Alonso, Catal. Lett. 86 (2003) 257.
[10] H. Nava, F. Pedraza, G. Alonso, Catal. Lett. 99 (2005) 65.
[11] H. Farag, K. Sakanishi, M. Kouzu, A. Matsumura, Y. Sugimoto, I. Saito, J. Mol. Catal. A: Chem. 206 (2003) 399.
[12] Y. Iwata, K. Sato, T. Yoneda, Y. Miki, Y. Sugimoto, A. Nishijima, H. Shimada, Catal. Today 45 (1998) 353.
[13] E. Devers, P. Afanasiev, B. Jouguest, M. Vrinat, Catal. Lett. 82 (2002) 13.
[14] C.S. Song, Y. Yoneyama, M.R. Kondam, US Patent No. 6451729, Method for preparing a highly active, unsupported high surface area MoS_2 catalyst, 2002.
[15] Y. Yoneyama, C.S. Song, Catal. Today 50 (1999) 19.
[16] Y. Yoneyama, C.S. Song, Energy Fuel 16 (2002) 767.
[17] K. Ramanathan, S. Weller, J. Catal. 95 (1985) 249.
[18] R. Frety, M. Breysse, M. Lacroix, M. Vrinat, Bull. Soc. Chim. Belg. 93 (1984) 697.

[19] G. Alonso, G. Berhault, A. Aguilar, V. Collins, C. Ornelas, S. Fuentes, R.R. Chianelli, J. Catal. 208 (2002) 359.
[20] M.H. Siadati, G. Alonso, B. Torres, R.R. Chianelli, Appl. Catal. A: Gen. 305 (2006) 160.
[21] L.S. Byskov, B. Hammer, J.K. Norskov, B.S. Clausen, H. Topsoe, Catal. Lett. 47 (1997) 177.
[22] J.H. Kim, X. Ma, C.S. Song, Y. Lee, S.T. Oyama, Energy Fuel 19 (2005) 353.
[23] O. Weisser, S. Landa, Sulphide Catalysts: Their Properties and Applications, Pergamon, Oxford, 1973, p. 91.
[24] J. Brito, M. Ilija, P. Hernandez, Thermochim. Acta 256 (1995) 325.
[25] K. Inamura, R. Prins, J. Catal. 147 (1994) 515.
[26] P. Afanasiev, Appl. Catal. A: Gen. 303 (2006) 110.
[27] B. Scheffer, N.J.J. Dekker, P.J. Mangnus, J.A. Moulijn, J. Catal. 121 (1990) 310.
[28] R.C. Hoodless, R.B. Moyes, P.B. Wells, Bull. Soc. Chim. Belg. 93 (1984) 673.
[29] C.J.H. Jacobsen, E. Tornqvist, H. Topsoe, Catal. Lett. 63 (1999) 179.
[30] X.S. Li, Q. Xin, X.X. Guo, P. Grange, B. Delmon, J. Catal. 137 (1992) 385.
[31] J.K. Norskov, B.S. Clausen, H. Topsoe, Catal. Lett. 13 (1992) 1.
[32] P. Raybaud, J. Hafner, G. Kresse, S. Kasztelan, H. Toulhoat, J. Catal. 190 (2000) 128.
[33] N.Y. Topsoe, H. Topsoe, J. Catal. 84 (1983) 386.
[34] O. Sorensen, B.S. Clausen, R. Candia, H. Topsoe, Appl. Catal. A: Gen. 13 (1985) 363.
[35] R.R. Chianelli, A.F. Ruppert, S.K. Behal, B.H. Kear, A. Wold, R. Kershaw, J. Catal. 92 (1985) 56.
[36] B. Delmon, Surf. Rev. Lett. 2 (1995) 25.
[37] P. Grange, Catal. Today 36 (1997) 375.
[38] B.C. Gates, H. Topsoe, Polyhedron 16 (1997) 3213.
[39] R. Prins, in: G. Ertl, H. Knozinger, J. Weitkamp (Eds.), Handbook of Heterogeneous Catalysis, vol. 4, Wiley-VCH, Berlin, 1997, p. 1909.
[40] V. Meille, E. Schulz, M. Lemaire, M. Vrinat, J. Catal. 170 (1997) 29.
[41] F. Bataille, J.L. Lemberton, P. Michaud, G. Perot, M. Vrinat, M. Lemaire, E. Schulz, M. Breysse, S. Kasztelan, J. Catal. 191 (2000) 409.
[42] A. Muller, E. Krickemeyer, R. Jostes, H. Bogge, E. Diemann, U. Bergmann, J. Chem. Sci. 406 (1985) 1715.
[43] H. Topsoe, B.S. Clausen, N. Topsoe, E. Pedersen, W. Niemann, A. Miiller, H. Bogge, B. Lengeler, J. Chem. Soc. Faraday Trans. 83 (1987) 2157.
[44] M. Breysse, G. Berhault, S. Kasztelan, M. Lacroix, F. Mauge, G. Perot, Catal. Today 66 (2001) 15.
[45] T. Kabe, A. Ishihara, Q. Zhang, Appl. Catal. A: Gen. 97 (1993) 1.
[46] J. Mijoin, V. Thevenin, N. Garcia Aguirre, H. Yuze, J. Wang, W.Z. Li, G. Perot, J.L. Lemberton, Appl. Catal. A: Gen. 180 (1999) 95.
[47] J.H. Kim, X. Ma, A. Zhou, C.S. Song, Catal. Today 111 (2006) 74.
[48] X. Ma, K. Sakanishi, T. Isoda, I. Mochida, Energy Fuel 9 (1995) 33.